

RI 9537

RI 9537

REPORT OF INVESTIGATIONS/1995

PLEASE DO NOT REMOVE FROM LIBRARY

LIBRARY
SPOKANE RESEARCH CENTER
RECEIVED

APR 14 1995

US BUREAU OF MINES
E. 315 MONTGOMERY AVE.
SPOKANE, WA 99207

Relative Self-Heating Tendencies of Coal, Carbonaceous Shales, and Coal Refuse

By Ann G. Kim

UNITED STATES DEPARTMENT OF THE INTERIOR



BUREAU OF MINES



U.S. Department of the Interior
Mission Statement

As the Nation's principal conservation agency, the Department of the Interior has responsibility for most of our nationally-owned public lands and natural resources. This includes fostering sound use of our land and water resources; protecting our fish, wildlife, and biological diversity; preserving the environmental and cultural values of our national parks and historical places; and providing for the enjoyment of life through outdoor recreation. The Department assesses our energy and mineral resources and works to ensure that their development is in the best interests of all our people by encouraging stewardship and citizen participation in their care. The Department also has a major responsibility for American Indian reservation communities and for people who live in island territories under U.S. administration.

Report of Investigations 9537

Relative Self-Heating Tendencies of Coal, Carbonaceous Shales, and Coal Refuse

By Ann G. Kim

**UNITED STATES DEPARTMENT OF THE INTERIOR
Bruce Babbitt, Secretary**

**BUREAU OF MINES
Rhea L. Graham, Director**

International Standard Serial Number
ISSN 1066-5552

CONTENTS

	<i>Page</i>
Abstract	1
Introduction	2
Oxidation of carbonaceous materials	2
Experimental method	4
Results	6
Summary	19
References	20
Appendix.—Nomenclature and equations	21

ILLUSTRATIONS

1. Rates of heat loss and heat gain as function of temperature	3
2. Standard differential thermal analysis	4
3. Normal crossing point temperature method	5
4. Tube furnace-differential thermal analyzer	5
5. Sample holder with thermocouple for determination of sample temperature	5
6. Modified crossing point-differential temperature method	7
7. Frequency distribution of measured heating rates at temperature levels 1, 2, and 3	9
8. Frequency distribution of calculated rates	9
9. Cumulative probability distribution for calculated heating rates	10
10. Self-heating probability values for all samples	12
11. Difference in measured sample heating rates in moist and dry air	12
12. Difference in measured maximum sample temperatures in moist and dry air	13
13. Initial oxygen depletion	15
14. Self-heating probability value versus initial oxygen depletion	16
15. Self-heating probability value versus average oxygen depletion	16
16. Carbon dioxide and carbon monoxide production as function of oxygen consumption	17
17. Self-heating probability values versus oxygen reaction rate	17
18. Self-heating probability values versus oxygen reaction mass rate	18
19. Self-heating probability values versus rate of oxygen adsorption	18
20. Self-heating probability values versus mass rate of oxygen adsorption	19

TABLES

1. Proximate analysis, total sulfur and heating value	6
2. Measured heating rates at temperature levels 1, 2, and 3	8
3. Calculated heating rates, mean heating rate, and calculated probability value	8
4. Measured maximum temperature difference at temperature levels 1, 2, and 3	8
5. Calculated temperature difference, mean maximum temperature difference, and calculated probability value	11
6. Calculated probability values for heating rate and maximum temperature difference, and self-heating probability value	11
7. Correlation coefficients for regression analyses	13
8. Average oxygen consumption	14
9. Carbon dioxide concentration at temperature levels 1, 2, and 3	14
10. Carbon monoxide concentration at temperature levels 1, 2, and 3	14
11. Change in sample weight during heating	15

UNIT OF MEASURE ABBREVIATIONS USED IN THIS REPORT

Btu	British thermal unit	kcal/mol	kilocalorie per mole
Btu/lb	British thermal unit per pound	min	minute
cal/s	calorie per second	mmol	millimole
cm	centimeter	mmol/kg	millimole per kilogram
cm ³	cubic centimeter	mmol/kg min	millimole per kilogram per minute
cm ³ /s	cubic centimeter per second	mmol/min	millimole per minute
g	gram	s	second
h	hour	°C	degree Celsius
kcal/g	kilocalorie per gram	°C/h	degree Celsius per hour
kcal/kg	kilocalorie per kilogram	°K	degree Kelvin

Reference to specific products does not imply endorsement by the U.S. Bureau of Mines.

RELATIVE SELF-HEATING TENDENCIES OF COAL, CARBONACEOUS SHALES, AND COAL REFUSE

By Ann G. Kim¹

ABSTRACT

Studies on the initiation and propagation of mine fires have dealt almost exclusively with coal. It has been assumed that the self-heating potential of carbonaceous shales and coal wastes is relatively low. However, in abandoned coal mines and waste banks, initiation and propagation of fires may be strongly dependent on the self-heating tendency of these materials. The purpose of this study was to compare the self-heating probability of carbonaceous shales and coal wastes to that of coals.

This study utilized a modified differential thermal analysis method, in which the combustion furnace temperature was the reference to which the sample temperature was compared. Based on the distribution of the maximum temperature differential and the sample heating rate, a self-heating probability value (SHPV) was calculated that corresponded to observed self-heating behavior. In this study, several of the carbonaceous shales and one coal waste had relatively high SHPV. The SHPV did not correspond directly to heating values or to differences in sulfur concentration.

¹Supervisory physical scientist, U.S. Bureau of Mines, Pittsburgh Research Center, Pittsburgh, PA.

INTRODUCTION

The Environmental Technology Group at the U.S. Bureau of Mines' (USBM) Pittsburgh Research Center has studied the detection and control of fires in abandoned mines and waste banks. Such fires present serious safety and environmental hazards (1-2).² When observable evidence of another ignition source is lacking, spontaneous combustion is frequently considered the probable cause of a fire in an abandoned mine, even though the particular coal may have exhibited a low susceptibility to spontaneous combustion during active mining. The discontinuous propagation of fires in abandoned mines also indicates that self-heating may be a factor. In many fire control projects at abandoned mines, evidence of the fire is found in the roof coal, indicating that the roof coal and shale may serve as a means for spreading the fire. Fires also occur in abandoned coal waste piles (3) that can contain both mine reject and prep plant waste. The subsurface location of combustion zones and the lack of an overt ignition source is evidence that self-heating is a factor in the initiation and propagation of these fires.

If the self-heating tendency of roof coals and associated carbonaceous shales is a parameter in how fires are spread

in abandoned coal mines, it has a direct bearing on the application of fire control techniques. If fires start or are spread along roof coals and shales, then any method which is directed toward controlling a fire in the mine void will not be effective (4). For instance, methods using the heat transfer capabilities of water or other agent depend on delivering the agent to a heated zone. If the heated zone exists in the roof of the mine, any procedure which delivers the agent to the mine floor is biased toward failure.

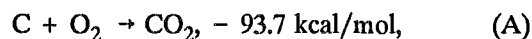
The objective of this study was to determine if the self-heating tendencies of carbonaceous shales and coal wastes were comparable to that of coal. To determine some characteristic thermal behavior that could be related to the probability of self-heating, the heating rate, and extent of heating were measured for each sample. To differentiate heat contributions from oxidation and from surface adsorption of moisture, heating behavior was determined in both dry and moist air. A self-heating probability value (SHPV), based on all temperature data, was then calculated for each sample within a random sample population and compared to observed self-heating.

OXIDATION OF CARBONACEOUS MATERIALS

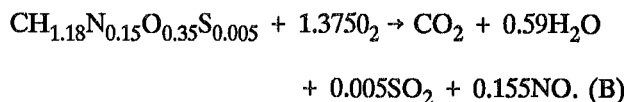
Coal is defined as "a readily combustible rock containing more than 50% by weight and 70% by volume of carbonaceous material...(5)." The noncarbonaceous matter in coal, mineral matter, is the inorganic noncombustible compounds that forms ash. According to American Society for Testing and Materials (ASTM) standards (6), the lowest rank coals have more than 48% fixed carbon and a heating value of less than 4,610 kcal/kg (8,300 Btu/lb). Carbonaceous shales are sedimentary rocks that probably developed from peats containing less than 50% organic material (7). Coal refuse consists of waste coal, slate, carbonaceous shales, pyritic shales, and clay associated with the coal seam and separated from the coal during the coal-cleaning process. The combustible content of this material averages between 1,110 and 3,330 kcal/kg (2,000 and 6,000 Btu/lb).

A fire, including those in abandoned mines and waste-banks, requires three elements: fuel, oxygen, and an ignition source. In coal combustion, the fuel is the carbon in

the coal. If combustion is considered the exothermic oxidation of carbon to form carbon dioxide, written as



the amount of heat liberated is approximately 8 kcal/g of carbon. However, coal is not composed of elemental carbon. On a dry, mineral matter free basis, coal contains between 60% and 90% carbon. The rest of the coal "molecule" is composed of hydrogen, oxygen, nitrogen, and sulfur. A general stoichiometric combustion reaction (8) can be written as:



This reaction is exothermic, producing from 5 to 10 kcal/g of coal, depending on the rank of the coal.

As coal oxidation occurs, the rate of reaction is a function of the temperature. Changes in the temperature of the coal are related to the difference between the rate of

²Italic numbers in parentheses refer to items in the list of references preceding the appendix at the end of this report.

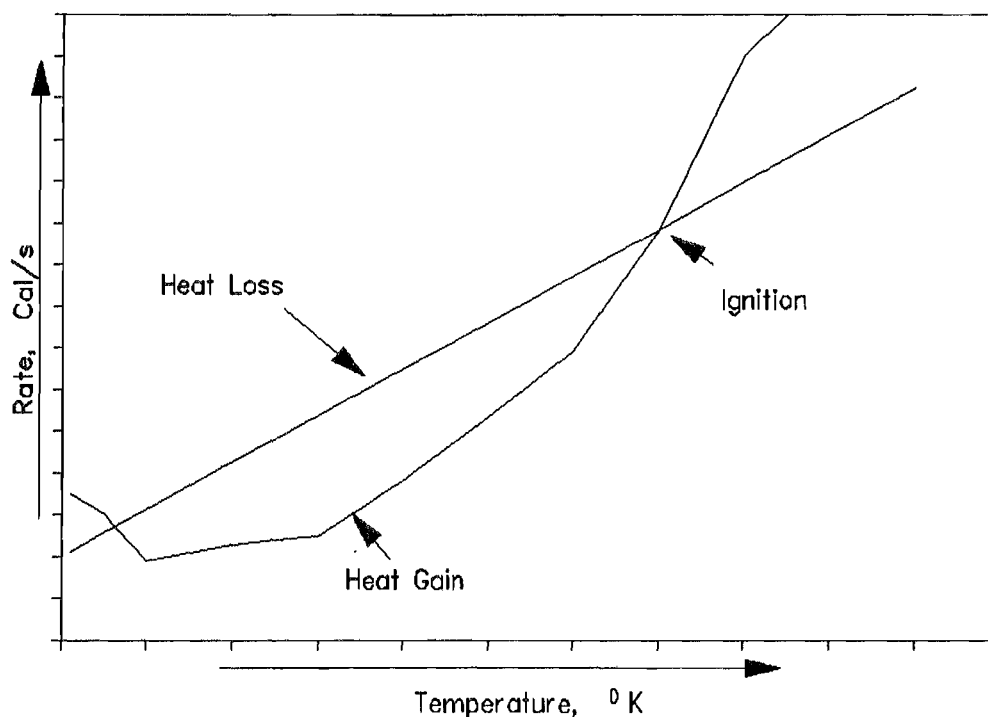
heat gain and the rate of heat loss. When these processes occur at the same rate, the temperature of the coal remains constant. When the rate of heat gain is greater than the rate of heat loss, the temperature of the reacting system increases. The rate of heat gain, which is related to reaction rate, heat capacity and heat transfer coefficient, is an exponential function of temperature and the rate of heat loss is a linear function of temperature. As the temperature increases, the rate of heat gain increases faster than the heat loss rate (figure 1). Ignition or self-sustaining combustion, will occur when the rate of heat generation exceeds the rate of heat loss (9). Ignition is, therefore, a function of the *amount* of energy released by a reaction and the *rate* at which it is released, as well as the rate at which energy is transferred from the reacting mass to the surroundings. The reaction rate is a function of the concentration of reactants, carbon and oxygen, the surface area, particle size, temperature, and activation energy.

In spontaneous ignition, there is no external heat source; natural reactions supply sufficient energy to sustain combustion. Spontaneous combustion in coal, carbonaceous shales, or coal refuse is related to the oxidation of

the coal to form CO_2 and CO . The oxidation of pyrite and the adsorption of water on the coal surface are also exothermic or heat generating processes. Although the normal ignition temperature for coal is between 420°C and 480°C , under adiabatic conditions (all heat generated is retained in the sample), the minimum temperature at which a coal will self-heat is 35°C to 140°C (10). In most abandoned mines and waste piles, conditions favor the retention of heat. Heat is typically lost by convection or conduction. In the essentially stagnant atmosphere of abandoned mines and waste piles, convection accounts for very little heat loss. Most heat transfer is probably by conduction to surrounding strata. Since rocks tend to be good insulators, the rate of heat loss in a mine or waste bank is relatively low.

Although spontaneous combustion of coal has been extensively studied (11), studies of self-heating of coal refuse have been limited, and there is almost no information dealing with the self-heating tendency of roof coals or carbonaceous shales associated with coals. The purpose of this study was to determine the tendency of such materials to self-heat relative to coals of moderate and high self-heating potential.

Figure 1



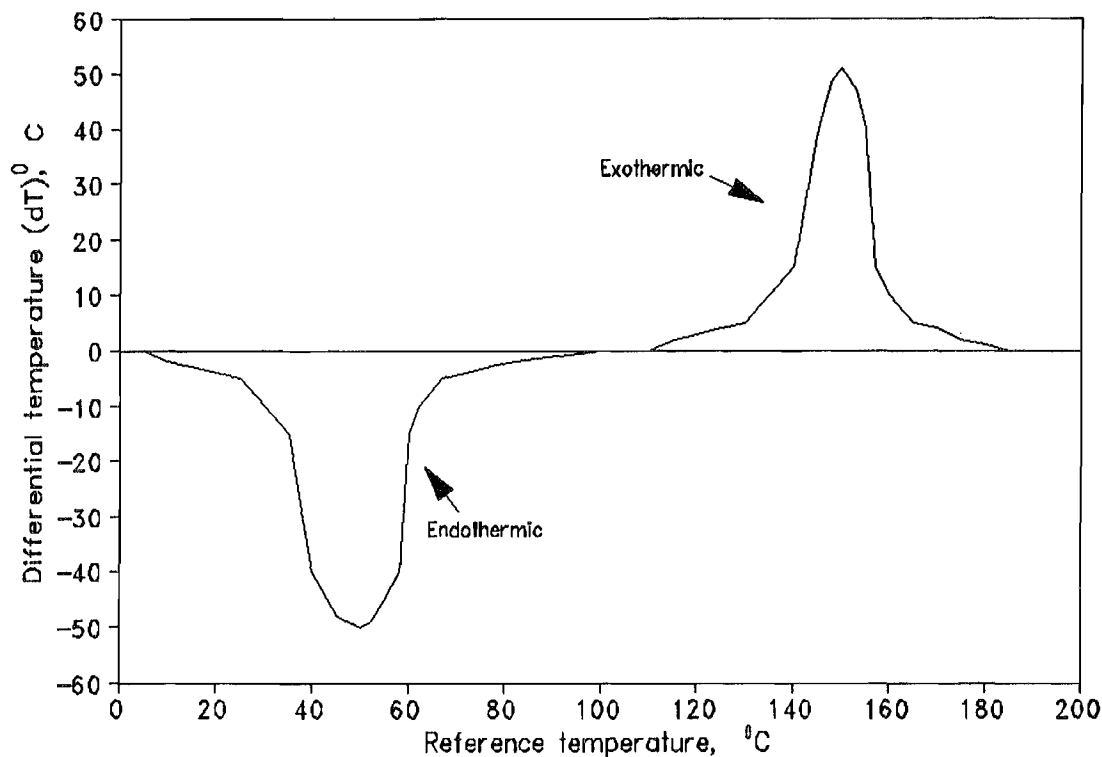
Rates of heat loss and heat gain as function of temperature.

EXPERIMENTAL METHOD

To determine the relative self-heating tendencies of coals, coal wastes and carbonaceous shales, a combination of differential thermal analysis and crossing point method was used. In standard differential thermal analysis, a temperature difference is measured between a sample and a standard (12). There are two compartments within a thermal block, one filled with the sample, the other filled with a reference material, usually sand. The block is heated at a constant rate and the temperature difference (dT) between the two materials is measured versus the temperature (T) of the reference (figure 2). Generally, sample size is of the order of a few grams, the atmosphere is stagnant, and heat loss is minimal. In the crossing point method, the rates at which the temperatures of a sample and a reference increase are compared (13). The point at which the temperatures of the sample equals the temperature of the standard (crossing point) is considered an indicator of the sample's tendency to self-heat (figure 3).

In the USBM study, the rate at which the sample temperature approached the reference temperature and the maximum difference between the sample and the reference were measured as indicators of self-heating behavior. A large sample (1,300-3,000 g) was heated in normal air in a 20-cm diameter tube furnace (figure 4). The furnace temperature was the reference temperature. The furnace was heated to 100 °C (T_{f1}) and held at that temperature for approximately 24 h. The temperature of the sample increased until it equaled or exceeded the furnace temperature. The rate ($RATE_1$) at which the sample temperature (T_{s1}) approached the furnace temperature (T_{f1}) and the difference between the furnace and maximum sample temperatures ($TEMP_1$) were measured. The furnace temperature was then raised to 150 °C (T_{f2}), and the procedure was repeated. On the third day the temperature of the furnace was raised to 200 °C (T_{f3}), and held at that level for 24 h.

Figure 2



Standard differential thermal analysis.

Figure 3

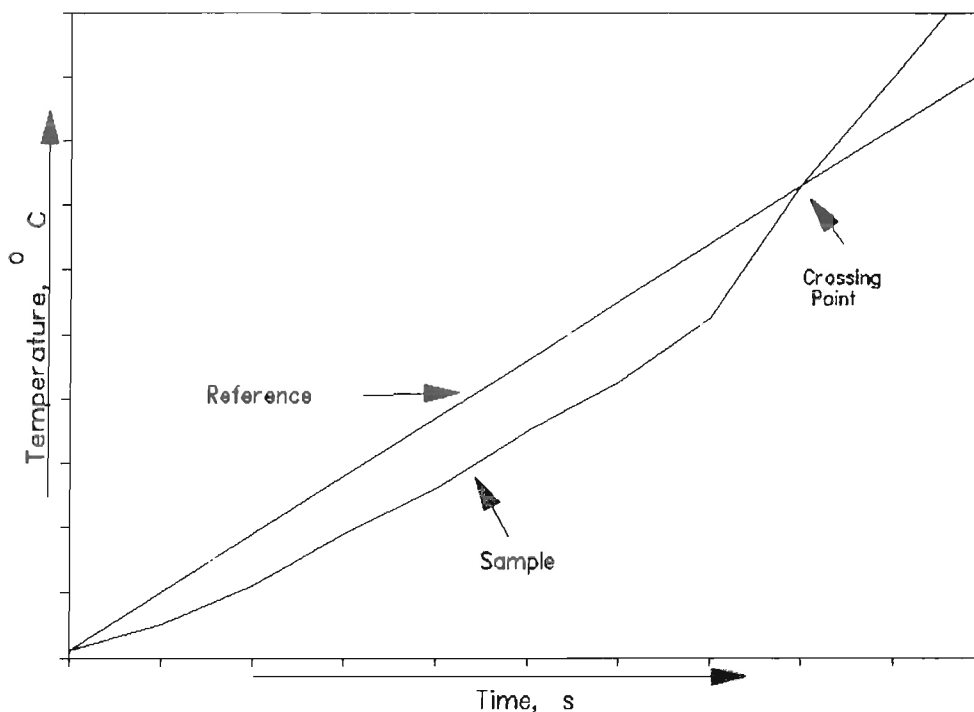
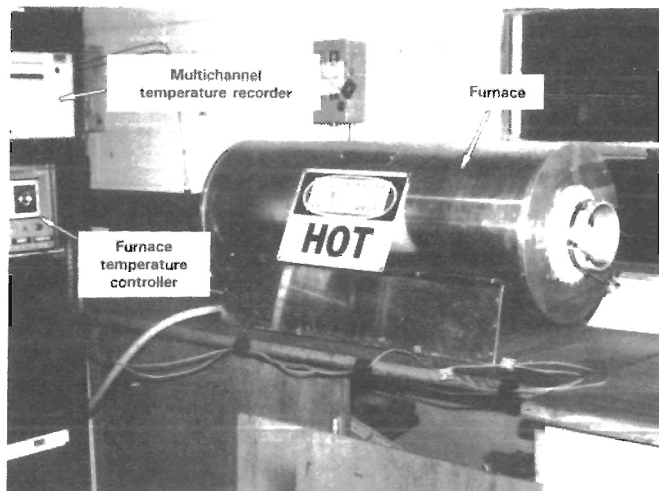
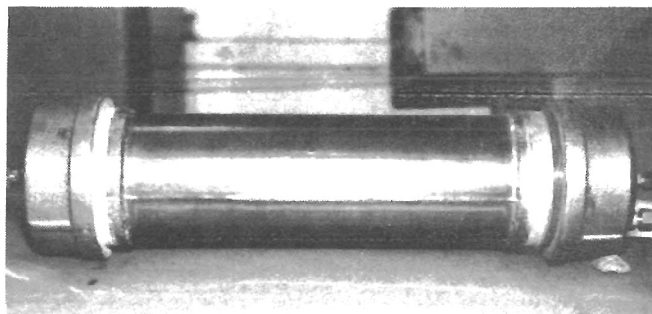
*Normal crossing point temperature method.*

Figure 4

*Tube furnace-differential thermal analyzer.*

In this study, the sample was crushed and screened to -0.6 cm by $+20$ mesh, then dried overnight under nitrogen at 100°C to remove surface moisture and reduce the effect of evaporative cooling. The sample container (figure 5) was a stainless steel cylinder with a volume of

Figure 5

*Sample holder (46 cm length, 10 cm ID) with thermocouple (type K) for determination of sample temperature.*

$3,700\text{ cm}^3$. Movable grids were used to hold the sample in a packed bed. Both ends were closed with threaded caps. The air line and a thermocouple were inserted through the cap into the sample chamber. The sample container was designed to promote the even distribution of air through the sample and to minimize the effect of discontinuities between the furnace wall and the central thermocouple measuring the sample temperature. The airflow rate was $15\text{ cm}^3/\text{s}$. Duplicate tests were performed with wet and dry air. Dry air was obtained by passing compressed air

through a tube of Drierite. In the moist air tests, the air was bubbled through water immediately before it entered the furnace. The designation d or m indicates whether the test was made with dry or moist air.

A gas-sampling line was installed in the center of the sample tube. A small pump was used to purge the line through a T-connector, the side arm of which held a needle assembly. Gas samples were collected in vacutainers by puncturing the septum with the needle. Evolved gas analysis, including CO, CO₂, and O₂, was performed by gas chromatography against a standard. Oxygen depletion was calculated as the difference between the oxygen concentration in the effluent from the furnace and that in the influent air.

Proximate analyses, total sulfur and heating values are given in table 1. The F Seam and D Seam samples were lower rank Western coals that were known to self-heat.

The coal sample, Blue Creek, and the shales labeled A, B, C, and D were from a mine that was experiencing self-heating, apparently initiated in the layers of shale in the floor. The shales were channel samples taken from undercasts, with A being closest to the mine floor. The samples C1, C2, D1, and D2 were samples of the C and D layers from different areas of the mine. Based on the analyses, they are considered different samples. Albright was a refuse sample from a burning waste bank; no apparent cause of the fire had been determined. The Bailey sample was a near-surface sample from a wastebank that was not associated with fire. The sample of the Pittsburgh coal and Pittsburgh roof shale were obtained from the Bruce-ton Experimental Mine. The mixture samples were combinations of the D Seam and either Albright refuse or Pittsburgh roof shale.

Table 1.—Proximate analysis, total sulfur and heating value, as received

Sample			Proximate analyses, %				Sulfur, %	Heating value, Btu/lb
Name	ID	Type ¹	Moisture	Ash	Volatile matter	Fixed carbon		
Albright	A	R	4.79	57.50	12.17	25.53	7.34	4,606
Bailey	B	R	2.18	79.76	12.03	6.03	1.56	1,573
Blue Creek	BC	C	0.77	36.16	19.16	43.91	0.70	9,422
D Seam	D	C	7.90	5.60	36.20	50.30	NA	12,368
D/Albright	DA	M	3.75	40.54	23.31	32.40	2.76	7,101
D/Pgh roof	DPR	M	4.91	48.75	22.92	23.42	0.19	5,835
F Seam	F	C	9.14	4.04	40.86	45.96	0.51	11,918
Pittsburgh	P	C	1.40	4.76	37.36	56.48	1.01	14,205
Pgh. Roof	PR	S	2.14	87.42	8.26	2.18	0.43	532
Zone A	A1	S	0.31	79.96	17.66	5.07	0.29	1,573
Zone B	B1	S	0.64	59.98	15.20	27.18	0.46	5,925
Zone C1	C1	S	0.94	75.28	10.51	13.27	2.82	2,725
Zone C2	C2	S	1.28	61.7	14.16	22.83	4.36	4,684
Zone D1	D1	S	1.04	61.58	14.26	23.12	4.74	4,841
Zone D2	D2	S	1.30	21.92	22.85	53.93	4.69	1,160

NA Not available.

¹R, refuse; C, coal; M, mixture; S, shale.

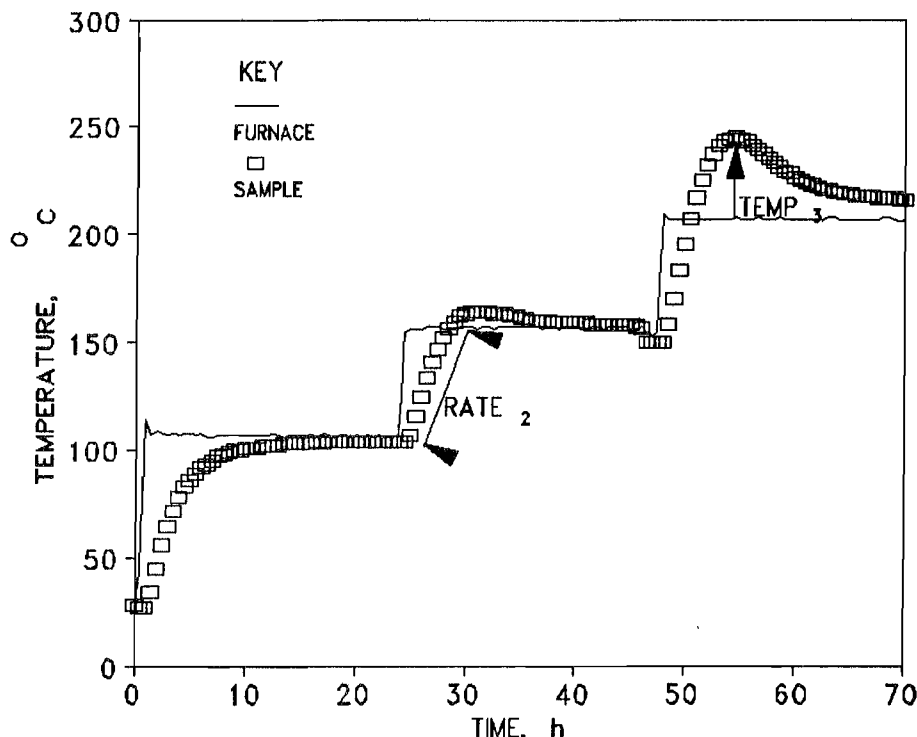
RESULTS

In this version of the crossing point method, the rate at which the sample temperature approaches the furnace temperature is considered a function of the rate at which the sample absorbs heat versus the rate at which heat is lost to the air flowing through the furnace. The extent to which the sample temperature exceeds the furnace temperature is assumed to be a function of the amount of heat generated by combustion reactions. Both values should be indicative of the tendency of the sample to self-heat. Heating rates and maximum temperatures were measured at the three furnace temperatures. The samples used in

this study were a heterogeneous collection of carbonaceous materials. If it is assumed that the tendency to self-heat is a function of some property of the samples and the selection of samples was representative, then the thermal behavior can be related to the tendency toward spontaneous combustion.

For each sample, the furnace temperature (T_{f1}) and the sample temperature (T_{s1}) were plotted against elapsed time (figure 6). At T_{f1} (100 °C), the temperature of the sample (T_{s1}) increased until it equaled or exceeded the furnace temperature. The temperature of the sample then

Figure 6



Modified crossing point-differential temperature method. Variation in furnace and sample temperatures with time. Albright Refuse in dry air (AR25d).

would return to the furnace temperature. This indicated sufficient heat generation to raise the sample temperature, followed by heat loss and cooling of the sample. The same pattern was observed at T_{i2} (150 °C). At 200 °C, some samples exhibited the previously observed heating-cooling cycle. However, for some samples, the temperature exceeded the furnace temperature and continued to increase, approaching the point of thermal runaway. If the sample temperature exceeded 300 °C, volatile coal tars would be distilled from the sample, and their deposition in the furnace and gas sampling lines would require extensive cleanup. If it seemed that uncontrolled heating of the sample would occur, the test was terminated after 8 h at T_{i3} .

The rate, $RATE_i$, at which the sample temperature increased was calculated for each temperature level (table 2).³ At T_{i1} , the mean heating rate for all samples was

7.4 °C/h, and the range was from 3.3 to 12.3 °C/h (figure 7). At T_{i2} , the mean heating rate was 10.3 °C/h, and the range was from 7.4 to 16.4 °C/h. At T_{i3} , the mean heating rate for all samples was 14.1 °C/h, and the range was from 10.0 to 18.3 °C/h.

Analysis of the rate data indicated that for all temperature levels (L), the measured rates ($RATE_L$) for each sample were generally related by a power of 1.5.

$$RATE_c = \frac{RATE_L}{(1.5)^{L-1}} \quad (1)$$

Using equation 1, standardized rate values, $RATE_c$, were calculated for all temperature levels (table 3), and plotted as a distribution (figure 8). Based on this distribution, a cumulative probability curve was constructed (figure 9), and a cumulative probability value (CPV_{RATE}) was obtained for each sample by plotting the mean ($RATE$) of the three $RATE_c$ values. As a cumulative probability function, all values were between 0 and 1, indicating the probability that the heating rate would be less than or equal to the

³In the following tables the samples are identified by a code in which the initial letters are the sample ID and type, listed in table 1. The numbers indicate a laboratory trial number and the last character indicates whether the sample was heated in dry or moist air.

RATE value. For example, the RATE value for sample PC28d was 5.97, for which the CPV_{RATE} was 0.351, indicating a 35% probability that the heating rate for this sample would reach the maximum rate observed for all samples. Sample FC24m had a RATE value of 9.29 and CPV_{RATE} of 0.919, indicating a greater than 90% probability that the heating rate for this coal would equal or exceed the maximum rate observed. On this basis, the F Seam coal, the D Seam coal, the Zone C, and Zone D shales had high probability values. The Blue Creek coal and the Albright waste also had relatively high values.

The maximum temperature differential, $TEMP_1$, between the furnace set temperature and the sample temperature was also determined for T_{f1} , T_{f2} , and T_{f3} (table 4). In those tests at level 3 that were terminated early due to sustained self-heating, the maximum temperature of the sample was calculated from the rate of heating at the time the test was terminated.

At T_{f1} , the mean temperature difference, $TEMP_1$, was 3.7 °C; the range was 0 to 10 °C. At T_{f2} , $TEMP_2$ was 17.4 °C; the range was 1 to 53 °C. At T_{f3} , $TEMP_3$ was 50.9 °C, and the range was 10 to 110 °C.

Table 2.—Measured heating rates ($RATE_1$) at temperature levels 1, 2, and 3, °C/h

Sample	$RATE_1$	$RATE_2$	$RATE_3$
AR25d	7.8	12.1	16.3
AR26m	7.9	10.4	15.6
A1S13d	8.8	9.2	13.1
A1S14m	7.9	7.4	11.1
BR11d	4.3	7.7	6.9
BR12m	ND	9.6	11.3
B1S15d	7.7	8.5	12.0
B1S17m	7.2	8.2	13.5
BCC30d	10.1	11.3	12.4
BCC29m	5.6	9.3	14.7
C1S16d	7.5	10.0	14.0
C1S18m	9.6	10.0	15.6
C2S22d	8.0	9.8	16.3
C2S21m	8.3	8.7	18.3
DC06m	6.3	15.0	ND
DC33m	5.1	15.6	18.2
D1S19d	9.3	8.0	13.6
D1S20m	8.0	10.0	14.6
D2S32d	7.4	11.8	17.5
D2S31m	9.5	10.2	18.0
ADM08m	4.5	10.5	ND
PRDM07m	3.3	8.5	ND
FC23d	ND	16.4	10.0
FC24m	12.3	14.7	13.0
PC28d	6.1	7.8	14.9
PC27m	6.0	8.7	12.7
PRS34d	6.5	8.7	15.0
Mean	7.4	10.3	14.1

ND Not determined.

Table 3.—Calculated heating rates, mean heating rate ($RATE$), and calculated probability value (CPV_{RATE})

Sample	$RATE_1$	$RATE_2/1.5$	$RATE_3/(1.5)^2$	$(RATE)$	CPV_{RATE}
AR25d	7.8	8.1	7.2	7.70	0.792
AR26m	7.9	6.9	6.9	7.26	0.661
A1S13d	8.8	6.1	5.8	6.92	0.579
A1S14m	7.9	4.9	4.9	5.92	0.343
BR11d	4.3	5.1	3.1	4.17	0.078
BR12m	NA	6.4	5.0	5.71	0.311
B1S15d	7.7	5.7	5.3	6.23	0.412
B1S17m	7.2	5.5	6.0	6.22	0.409
BCC30d	10.1	7.5	5.5	7.51	0.724
BCC29m	5.6	6.2	6.5	6.11	0.382
C1S16d	7.5	6.7	6.2	6.80	0.549
C1S18m	9.6	6.7	6.9	7.73	0.777
C2S22d	8.0	6.5	7.2	7.26	0.662
C2S21m	8.3	5.8	8.1	7.41	0.669
DC06m	6.3	10.0	NA	8.20	0.859
DC33m	5.1	10.4	8.1	7.87	0.826
D1S19d	9.3	5.3	6.0	6.89	0.573
D1S20m	8.0	6.7	6.5	7.05	0.611
D2S32d	7.4	7.9	7.8	7.68	0.765
D2S31m	9.5	6.8	8.0	8.10	0.848
ADM08m	4.5	7.0	5.7	5.51	0.281
PRDM07m	3.3	5.7	4.9	4.63	0.148
FC23d	NA	10.9	4.4	7.69	0.767
FC24m	12.3	9.8	5.8	9.29	0.919
PC28d	6.1	5.2	6.6	5.97	0.351
PC27m	6.0	5.8	5.6	5.81	0.327
PRS34d	6.5	5.8	6.7	6.32	0.434

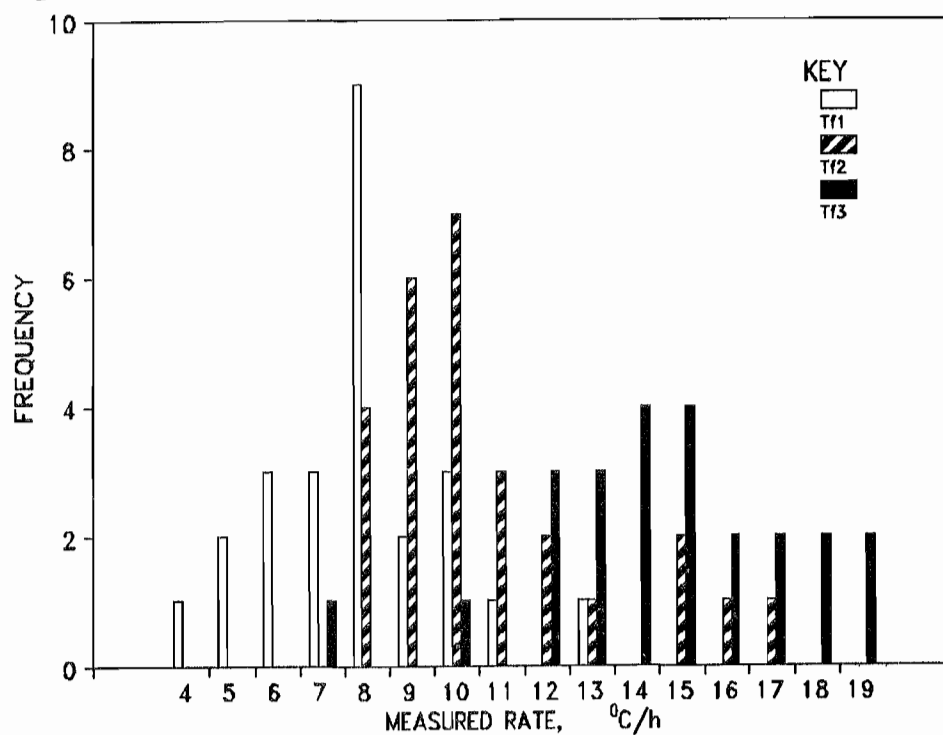
NA Not available.

Table 4.—Measured maximum temperature difference ($TEMP_1$) at temperature levels 1, 2, and 3, °C

Sample	$TEMP_1$	$TEMP_2$	$TEMP_3$
AR25d	4	14	45
AR26m	3	9	19
A1S13d	2	3	16
A1S14m	4	12	54
BR11d	1	7	22
BR12m	3	7	26
B1S15d	2	6	25
B1S17m	4	6	23
BCC30d	5	25	110
BCC29m	1	15	71
C1S16d	3	10	43
C1S18m	4	22	99
C2S22d	2	7	33
C2S21m	3	1	10
DC06m	10	53	NA
DC33m	7	48	70
D1S19d	3	5	24
D1S20m	3	11	56
D2S32d	3	14	56
D2S31m	3	20	83
ADM08m	4	25	NA
PRDM07m	3	21	NA
FC23d	9	56	95
FC24m	8	42	67
PC28d	1	10	63
PC27m	3	13	63
PRS34d	1	8	48
Mean	3.7	17.4	50.9

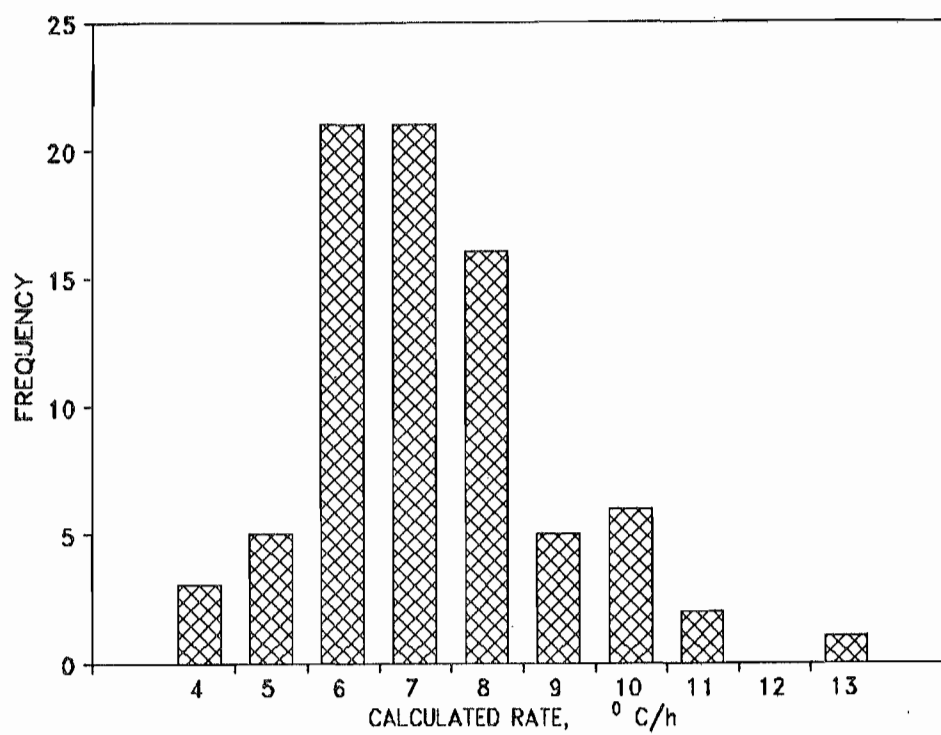
NA Not available.

Figure 7



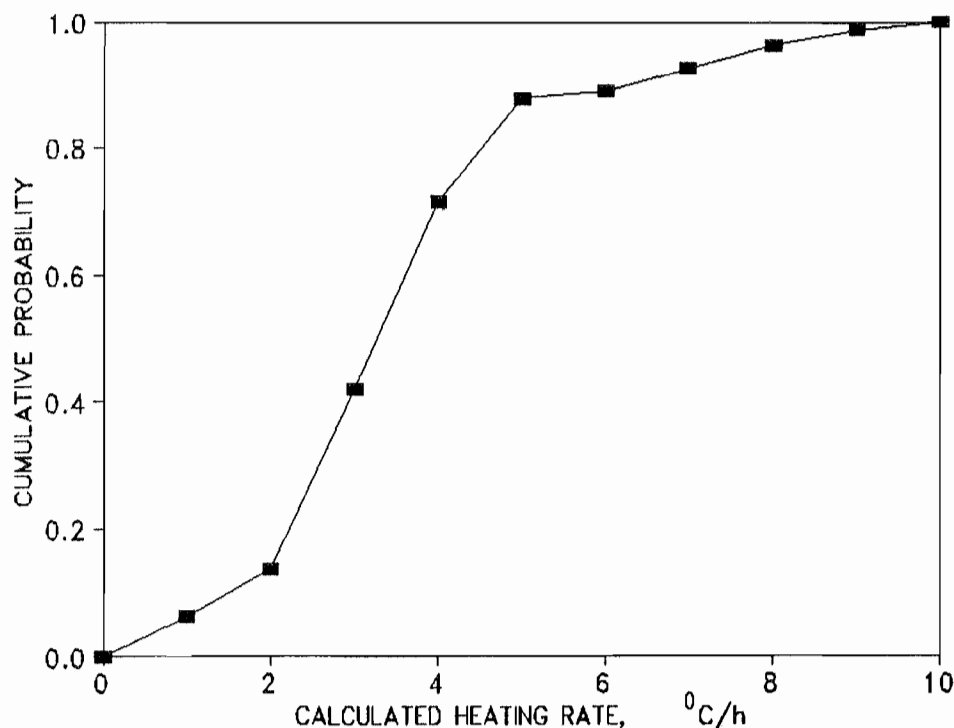
Frequency distribution of measured heating rates at temperature levels 1, 2, and 3.

Figure 8



Frequency distribution of calculated rates.

Figure 9



Cumulative probability distribution for calculated heating rates.

It was observed that the $TEMP_2$ and $TEMP_3$ values could be calculated as a function of T_{f1} . At T_{f1} ,

$$TEMP_c = TEMP_1. \quad (2)$$

At T_{f2} and T_{f3} ,

$$TEMP_c = \frac{\sqrt{T_L}}{(L - 1)}. \quad (3)$$

As with the rate data equations 2 and 3 were used to calculate $TEMP$ values (table 5). A frequency distribution of the $TEMP_c$ values, and $TEMP_{values}$ cumulative probability values (CPV_{TEMP}) were determined for each sample. The F Seam and Blue Creek coals in dry air, the F Seam, D Seam, Zone C1 shale, Zone D2 shale and the mixtures of D Seam coal in moist air all had relatively high values.

In general, CPV_{RATE} did not correspond directly with CPV_{TEMP} (table 6). However, the mean of these values, denoted as self-heating probability value (SHPV), was greater than 0.775 only for samples that had approached thermal runaway (figure 10). Since it could be correlated with observed self-heating, this value was considered an estimator of the probability that a given sample would self-heat.

The presence of moisture in the air stream has two possible effects. The exothermic adsorption of water on the sample surface is a mechanism for initiating self-heating and could raise the sample temperature in moist air. Water has a higher heat capacity than air and the moist air could absorb more heat than dry air, lowering the sample temperature. The effect of moisture on heating rate was apparently random across all temperature levels (figure 11). Only one sample (A1S) consistently heated faster in dry air. At T_{f2} , approximately half of the samples heated faster in dry air, and on the average there was less than 1 °C/h difference in heating rate. At T_{f2} , most of the samples heated more rapidly in dry air, although the average difference between wet and dry air heating rates was still less than 1 °C/h. At T_{f3} , almost all of the samples heated faster in moist air, and the average difference between dry and moist air was 1 °C/h. Differences in the rate of heating with temperature and with moisture may be related to relative changes in the heat capacities of the various materials. Heat capacity generally increases with temperature. However, in studies of the Pittsburgh coal (14) the heat capacity varied directly for dried coal samples, but, for samples containing moisture, it increased to a maximum at 125 °C, then decreased.

Table 5.—Calculated temperature difference, mean maximum temperature difference $\overline{\text{TEMP}}$, and calculated probability value (CPV_{TEMP})

Sample	TEMP ₁	SQRT(TEMP ₂)	SQRT(TEMP ₃) 2	$\overline{\text{TEMP}}$	CPV_{TEMP}
AR25d	4	3.74	3.35	3.70	0.627
AR26m	3	3.00	2.18	2.72	0.342
A1S13d	2	1.73	2.00	1.91	0.129
A1S14M	4	3.46	3.67	3.71	0.631
BR11d	1	2.65	2.35	2.00	0.135
BR12M	3	2.65	2.55	2.73	0.344
B1S15D	2	2.45	2.50	2.32	0.226
B1S17m	4	2.45	2.40	2.95	0.405
BCC30d	5	5.00	5.24	5.08	0.878
BCC29m	1	3.87	4.21	3.03	0.428
C1S16d	3	3.16	3.28	3.15	0.463
C1S18m	4	4.69	4.97	4.56	0.805
C2S22d	2	2.65	2.87	2.51	0.279
C2S21m	3	1.00	1.58	1.86	0.125
DC06m	10	7.28	NA	8.68	0.980
DC33m	7	6.93	4.18	6.04	0.890
D1S19d	3	2.24	2.45	2.56	0.295
D1S20m	3	3.32	3.74	3.35	0.524
D2S32d	3	3.74	3.74	3.49	0.566
D2S31m	4	4.47	4.56	4.34	0.818
ADM08M	4	5.00	NA	4.51	0.798
PRDM07m	3	4.58	NA	3.82	0.662
FC23d	9	7.48	4.87	7.12	0.930
FC24m	8	6.48	4.09	6.19	0.896
PC28d	1	3.16	3.97	2.71	0.337
PC27m	3	3.61	3.97	3.52	0.575
PRS34d	1	2.83	3.46	2.43	0.258

Table 6.—Calculated probability values for heating rate (CPV_{RATE}) and maximum temperature difference (CPV_{TEMP}), and self-heating probability value (SHPV)

Sample	CPV_{RATE}	CPV_{TEMP}	SHPV
AR25d	0.792	0.627	0.710
AR26m	0.661	0.342	0.502
A1S13d	0.579	0.129	0.354
A1S14m	0.343	0.631	0.487
BR11d	0.078	0.135	0.107
BR12m	0.311	0.344	0.328
B1S15d	0.412	0.226	0.319
B1S17m	0.409	0.405	0.407
BCC30d	0.724	0.878	0.801
BCC29m	0.382	0.428	0.405
C1S16d	0.549	0.463	0.506
C1S18m	0.777	0.805	0.791
C2S22d	0.662	0.279	0.471
C2S21m	0.699	0.125	0.397
DC06m	0.859	0.980	0.920
DC33m	0.826	0.890	0.858
D1S19d	0.573	0.295	0.434
D1S20m	0.611	0.524	0.568
D2S32d	0.765	0.566	0.666
D2S31m	0.848	0.818	0.833
ADM08m	0.281	0.798	0.540
PRDM07m	0.148	0.662	0.405
FC23d	0.767	0.930	0.849
FC24m	0.919	0.896	0.908
PC28d	0.351	0.337	0.344
PC27m	0.327	0.575	0.451
PRS34d	0.434	0.258	0.346

The maximum temperature data were more consistent with respect to each sample, i.e., three of the samples had higher temperatures in dry air at all three temperature levels while six reached higher temperatures in moist air (figure 12). Self-heating was not correlated with the presence or absence of moisture. One sample (F Seam) self-heated in both moist and dry air; the C1 and D2 shales self-heated in moist air, but the Blue Creek coal self-heated in dry air. The adsorption of moisture apparently has a more pronounced effect on the self-heating behavior of lower rank coals and shales.

Relating SHPV with the tendency to self-heat and comparing it to the composition of the samples indicated no simple relationship. Regression analyses with the CPV_{RATE} , CPV_{TEMP} , and moisture content of the air as dependent variables and the ash, fixed carbon, sulfur, and BTU value as independent variables indicated relatively low correlations (table 7). When the SHPV for all samples was the dependent variable, the correlations to fixed carbon and BTU values were higher, but variations in these values still accounted for less than 50% of the variation in SHPV. The concentration of ash, either as received or dry, was the only compositional variable that had a correlation coefficient greater than 0.50. Less than 10% of the variation could be related to variations in sulfur concentration.

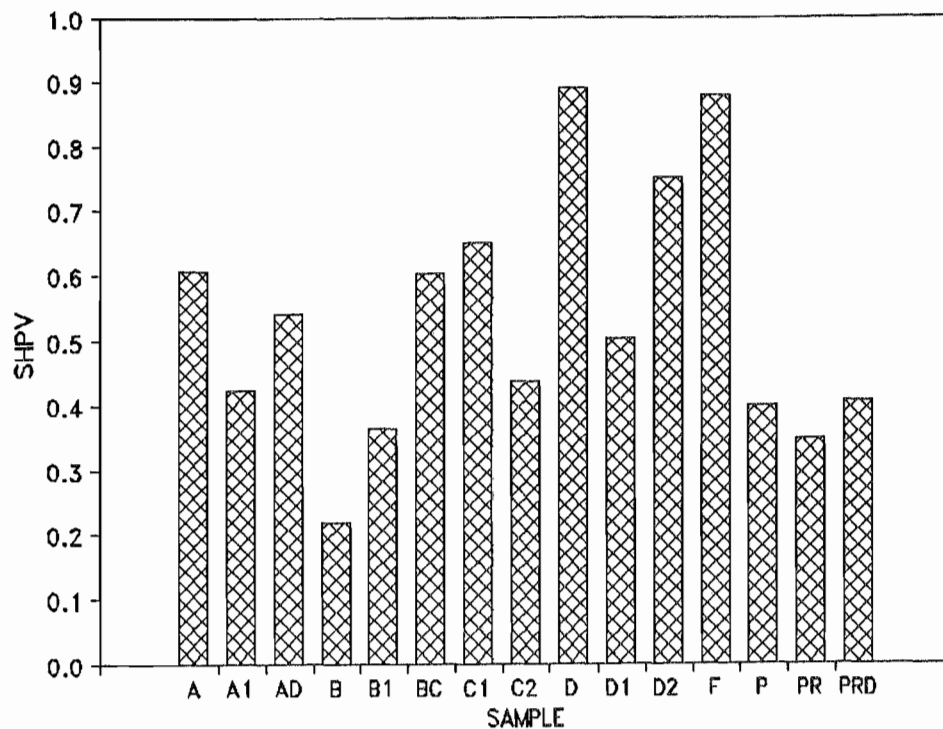
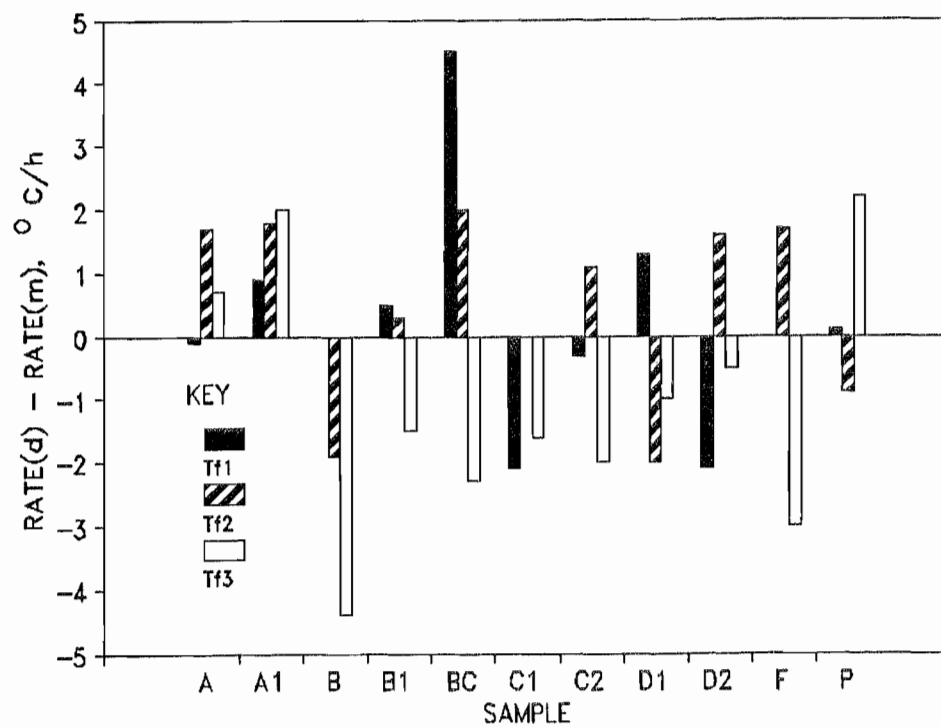
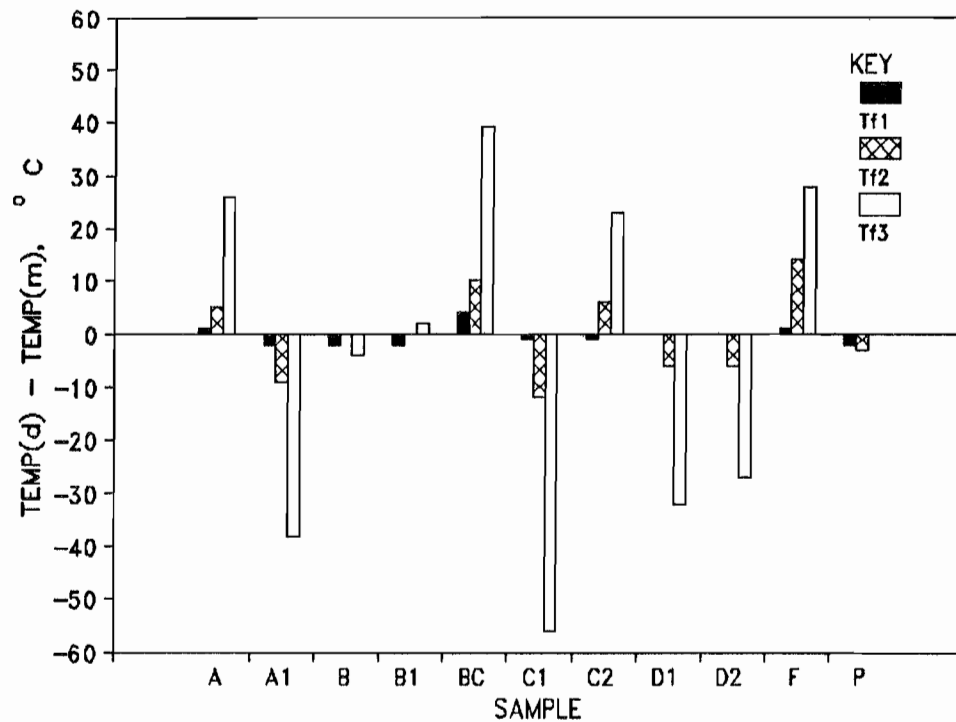
Figure 10**Self-heating probability values (SHPV) for all samples.****Figure 11****Difference in measured sample heating rates in moist and dry air at temperature levels 1, 2, and 3.**

Figure 12



Difference in measured maximum sample temperatures in moist and dry air at temperature levels 1, 2, and 3.

Table 7.—Correlation coefficients for regression analyses with composition factors as independent variables and calculated probability values as dependent variables

	← CPV _{RATE}	DRY CPV _{TEMP}	→ CPV _d	← CPV _{RATE}	MOIST CPV _{TEMP}	→ CPV _m	SHPV
Ash, AR	0.14	0.40	0.32	0.15	0.34	0.34	0.51
FC, AR	0.17	0.39	0.33	0.15	0.21	0.26	0.44
S, AR	0.19	0.01	0.07	0.08	0.13	0.01	0.01
BTU, AR	0.11	0.35	0.27	0.13	0.27	0.28	0.43
ASH, dry	0.14	0.39	0.31	0.16	0.35	0.35	0.51
FC, dry	0.18	0.42	0.36	0.17	0.24	0.30	0.49
S, dry	0.19	0.00	0.07	0.08	0.14	0.01	0.01
BTU, dry	0.12	0.38	0.29	0.15	0.30	0.32	0.47
FE, mmmf	0.24	0.28	0.31	0.12	0.01	0.03	0.20
S, mmmf	0.03	0.01	0.00	0.04	0.23	0.03	0.02
BTU, mmmf	0.16	0.29	0.27	0.11	0.06	0.11	0.29

mmmf moisture and mineral matter free.

The depletion of oxygen, ($-d[O_2]$) as well as, the amount of CO_2 and CO produced ($d[CO_2]$, $d[CO]$) were monitored as indicators of heat-producing chemical reactions. Both factors increase with increased temperature (tables 8-10) for each sample. The presence of moisture in the air stream has no consistent effect on the change in the concentration of oxygen.

Table 8.—Average oxygen consumption ($-d[O_2]$): at start of test (T_{f0}) and at temperature levels 1, 2, and 3

Sample	$-d[O_2]^1$, %			
	T_{f0}	T_{f1}	T_{f2}	T_{f3}
AR25d	12.76	3.94	8.62	13.78
AR26m	13.46	2.76	4.21	11.80
BR11d	4.70	1.21	2.21	5.38
BR12m	1.44	1.72	2.75	11.34
BCC30d	3.50	1.53	4.12	11.70
BCC29m	3.36	1.93	2.64	11.41
FC23d	18.46	1.09	5.00	8.61
FC24m	19.50	2.30	9.09	9.96
PC28d	2.30	2.94	3.10	14.75
PC27m	6.31	2.19	7.50	18.61
AlS13d	1.80	4.60	4.53	6.56
AlS14m	3.36	4.09	4.73	12.80
B1S15d	1.80	2.13	1.82	7.70
B1S17m	0.62	1.49	1.78	8.16
C1S16d	0.88	0.94	3.50	12.03
C1S18m	5.04	1.35	4.71	13.50
C2S22d	12.83	0.24	1.48	12.09
C2S21m	4.37	1.49	2.39	4.98
D1S19d	2.14	0.66	1.35	3.48
D1S20m	1.70	1.68	3.50	14.50
D2S32d	7.67	1.40	6.74	12.49
D2S31m	5.34	0.87	3.25	13.85
DCO6m	6.43	2.65	5.78	5.01
DC33m	1.11	1.67	6.66	10.65
ADM08m	1.27	2.1	5.53	8.33
PRDM07m	1.20	2.78	11.66	6.85
PRS34d	1.27	0.57	0.85	7.27

¹Difference between effluent and influent concentration.

Oxygen was apparently adsorbed on the sample when it was initially placed in the furnace ($t=0$; table 8). For more than half of the samples, the oxygen concentration decreased by less than 5% during the first 4 min in the furnace (figure 13). For 20 pct of the samples the oxygen concentration decreased by more than 10%. Initial oxygen depletion was not related to the self-heating probability (figure 14). When averaged over the three temperature levels, SHPV showed a general increase with greater oxygen depletion (figure 15). The physical adsorption of oxygen or the formation of carbon-oxygen compounds on the surface of the coal (15) may be related to the inequality in the O_2 , CO_2 , CO concentrations and to the increase in sample weight for some of the samples (table 11).

Table 9.—Carbon dioxide [CO_2] concentration at temperature levels 1, 2, and 3

Sample	$[CO_2]$, %		
	T_{f1}	T_{f2}	T_{f3}
AR25d	0.04	0.44	1.77
AR26m	0.06	0.16	1.42
BR11d	0.09	0.16	0.90
BR12m	0.03	0.19	2.22
BCC30d	0.04	0.35	4.13
BCC29m	0.03	0.26	2.47
FC23d	0.33	1.95	2.77
FC24m	0.28	1.38	1.81
PC28d	0.49	2.26	1.44
PC27m	0.08	0.35	4.34
A1S13d	0.10	0.07	0.81
A1S14m	0.06	0.48	2.25
B1S15d	0.02	0.11	1.11
B1S17m	0.04	0.19	1.31
C1S16d	0.02	0.26	1.96
C1S18m	0.05	0.36	3.00
C2S22d	0.02	0.18	1.94
C2S21m	0.02	0.06	1.26
D1S19d	0.02	0.13	0.72
D1S20m	0.04	0.25	2.24
D2S31m	0.04	0.72	2.19
D2S31m	0.03	0.30	2.50
DCO6m	0.53	2.18	1.84
DC33m	0.41	2.58	5.97
ADM08m	0.16	0.98	1.67
PRDM07m	1.29	3.44	1.82
PRS34d	0.08	0.07	1.77

Table 10.—Carbon monoxide [CO] concentration at temperature levels 1, 2, and 3

Sample	$[CO]$, %		
	T_{f1}	T_{f2}	T_{f3}
AR25d	ND	0.05	0.76
AR26m	ND	0.04	0.96
BR11d	ND	0.06	0.28
BR12m	ND	0.05	0.40
BCC30d	ND	0.19	1.04
BCC29m	0.01	ND	0.94
FC23d	ND	ND	0.89
FC24m	ND	0.51	0.45
PC28d	ND	0.04	0.59
PC27m	ND	0.06	1.86
A1S13d	ND	ND	0.21
A1S14m	ND	0.05	1.46
B1S15d	ND	0.01	0.42
B1S17m	ND	ND	0.41
C1S16d	ND	0.03	1.00
C1S18m	ND	0.09	1.95
C2S22d	ND	0.04	0.87
C2S21m	ND	ND	0.14
D1S19d	ND	ND	0.26
D1S20m	ND	0.04	0.94
D2S32d	ND	0.23	0.95
DCO6m	0.07	0.4	0.4
DC33m	0.02	0.36	1.67
ADM08m	0.02	0.23	0.48
PRDM07m	0.32	0.70	0.42
PRS34d	ND	ND	0.73
D2S31m	ND	0.08	1.00

ND Not Detected

Table 11.—Change in sample weight during heating

Sample	Weight, g		Change, %
	Before	After	
AR25d	2407	2466	+2.45
AR26m	2410	2380	-1.24
A1S14M	2848	2865	+0.60
AIS13d	3525	3525	0
BCC30d	2114	2114	0
BCC29m	2110	2090	-0.95
BR11d	3662	3569	-2.54
BR12m	3525	3393	-3.74
BIS17m	3201	3203	+0.06
B1S15d	3525	3525	0
C1S16d	3298	NA	
C1S18m	3208	3170	-1.18
C2S22d	2523	2527	+0.16
C2S21m	1990	2002	+0.60
D1S19d	3699	3704	-0.14
D1S20m	3100	3166	+2.13
D2S32d	2746	2731	-0.55
D2S31m	NA	NA	
DC06m	NA	NA	
DC33m	1844	1864	+1.08
ADM08m	2550	2536	-0.55
PRDM07m	2959	2911	-1.62
FC23d	1300	1243	-4.38
FC24m	1300	1243	-4.38
PC28d	1983	NA	
PC27m	2053	1948	-5.11
PRS34d	2959	2911	-1.62

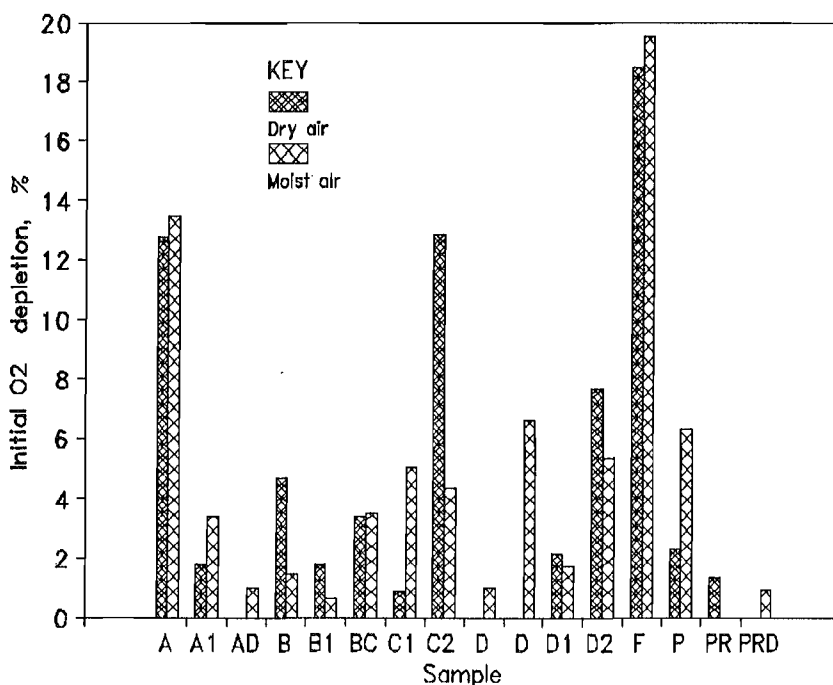
NA Not available

The production of CO_2 follows the same pattern as the consumption of O_2 . If the initial adsorption of oxygen is low, the initial production of CO_2 is also low; and if more oxygen is consumed initially, more CO_2 is produced initially. Although the production of CO_2 varies directly with the consumption of oxygen (figure 16), the amount of CO_2 produced is, on average, less than 25% of O_2 consumed. Carbon monoxide production is less than CO_2 production. At temperatures above 100 °C, the concentration of CO increases as the CO_2 concentration increases. At temperatures of 100 °C or less, the CO concentration is usually below the limits of detection (table 11). On the average, CO accounts for 7% of the reduction in O_2 concentration.

Oxygen depletion is the measured change in O_2 concentration between the influent and effluent air samples. Based on gas concentrations in millimoles, the reactant $[\text{O}_2]$ was calculated as the amount needed to produce the observed concentrations of CO_2 and CO. The adsorbed $[\text{O}_2]$ was the measured depletion minus the calculated reactant concentration. Comparing SHPV with the oxygen reaction rate indicates a linear trend (figure 17), although the correlation appears better when the reaction rate is related to the mass of the sample (figure 18).

The SHPV does not vary directly with the rate of O_2 adsorption (figure 19); however, the correlation improves when adsorption is related to the mass of the sample (figure 20). The samples with SHPV greater than 0.75 exhibit no dependence on oxygen adsorption rate.

Figure 13



Initial oxygen depletion ($-\text{d}[\text{O}_2]$). Gas samples taken within 5 min of start of test; average air residence time = 2.4 min.

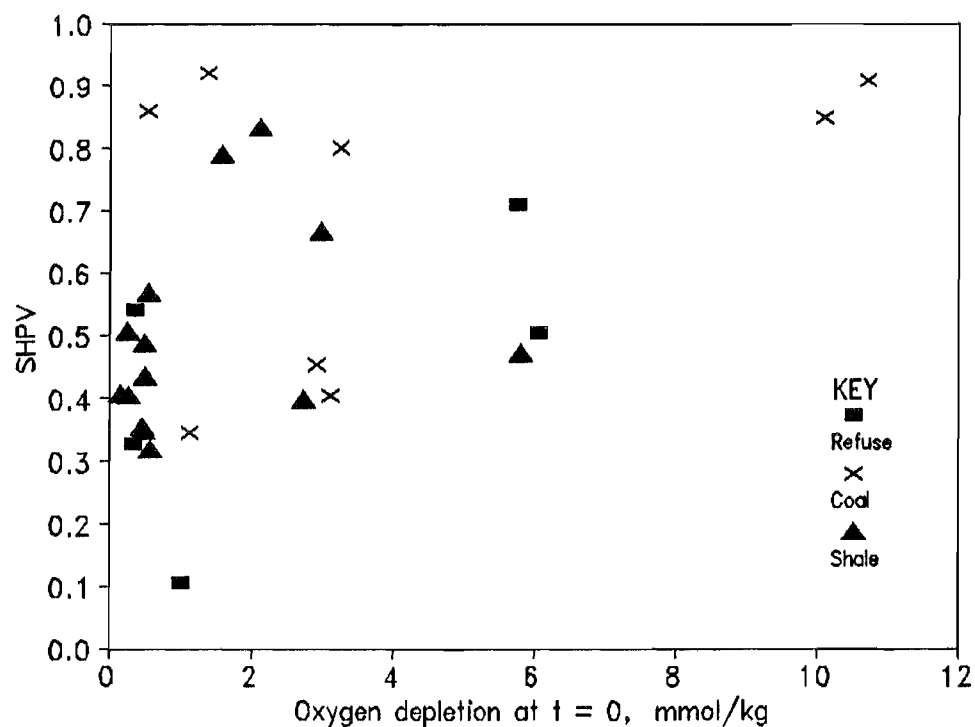
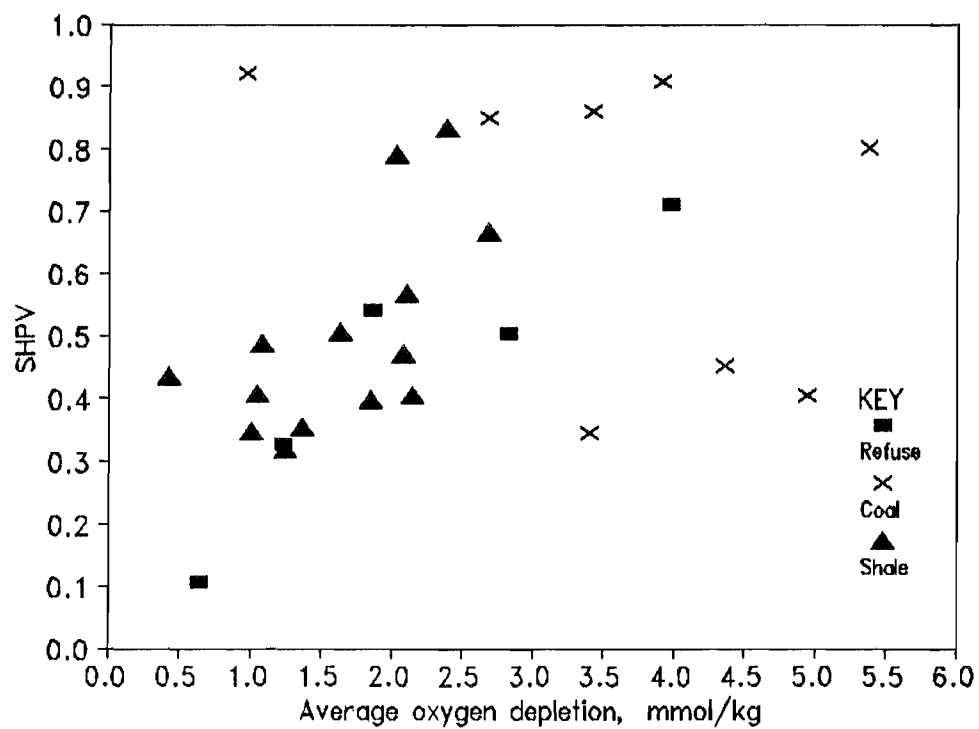
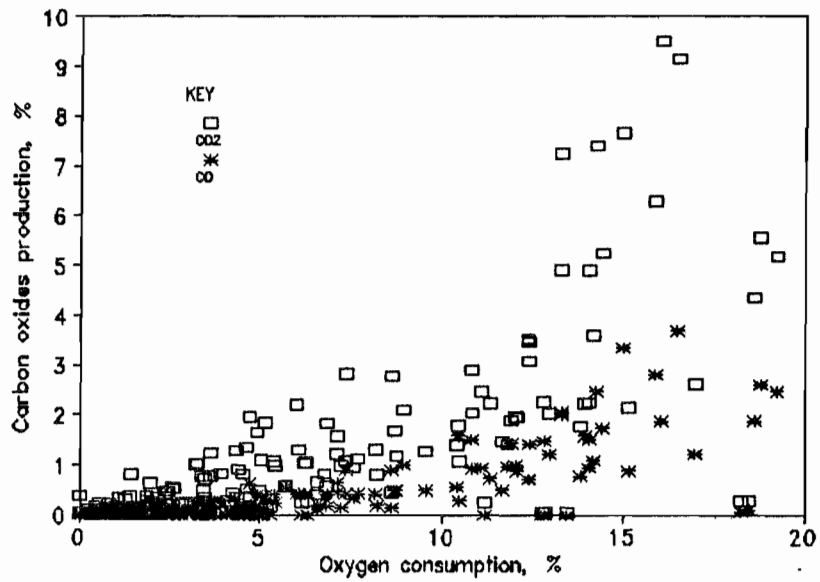
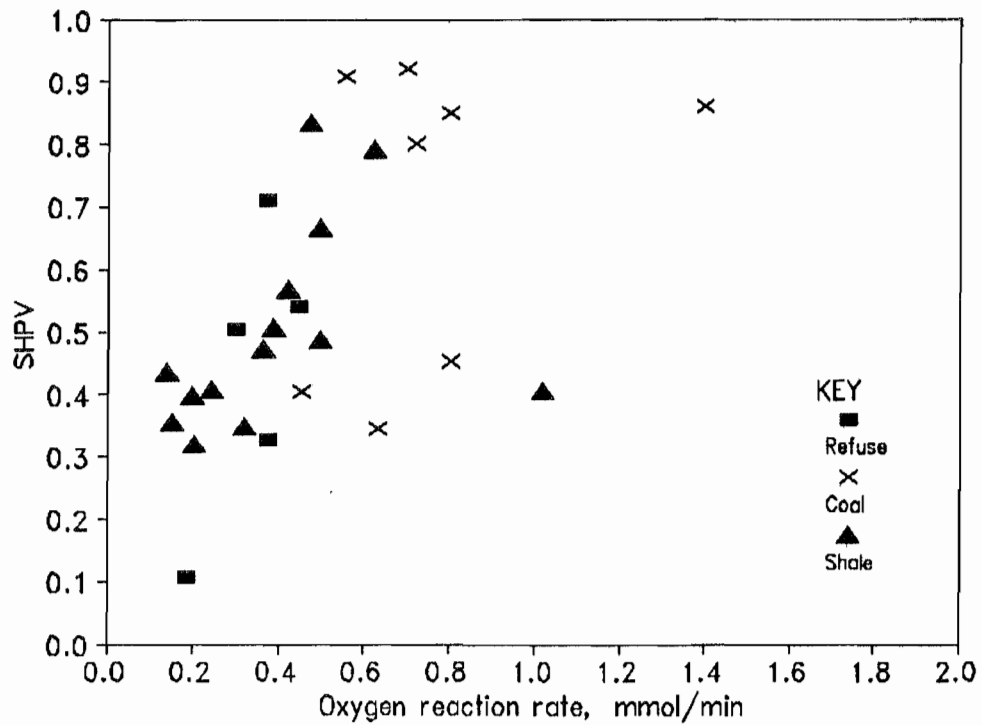
Figure 14**Self-heating probability value versus initial oxygen depletion.****Figure 15****Self-heating probability value versus average oxygen depletion.**

Figure 16

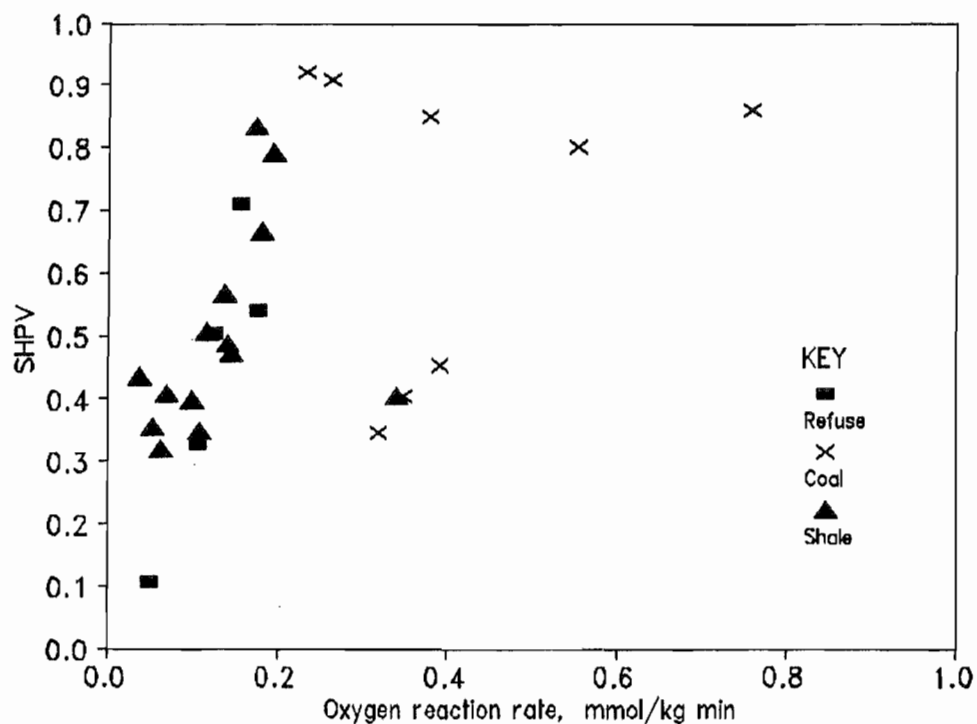


Carbon dioxide and carbon monoxide production as function of oxygen consumption.

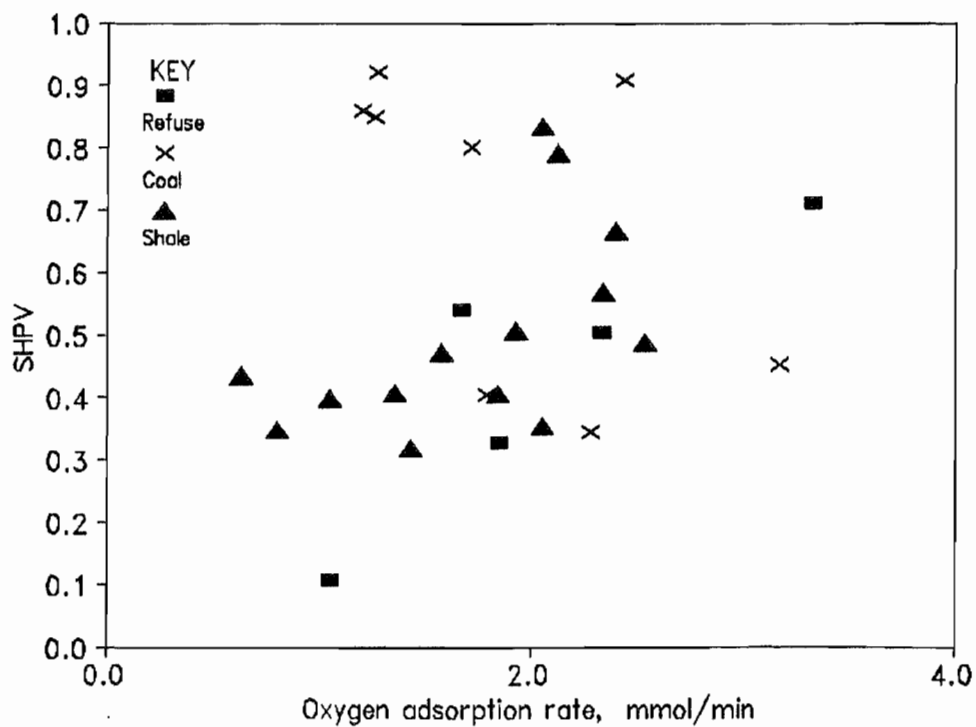
Figure 17



Self-heating probability values versus oxygen reaction rate.

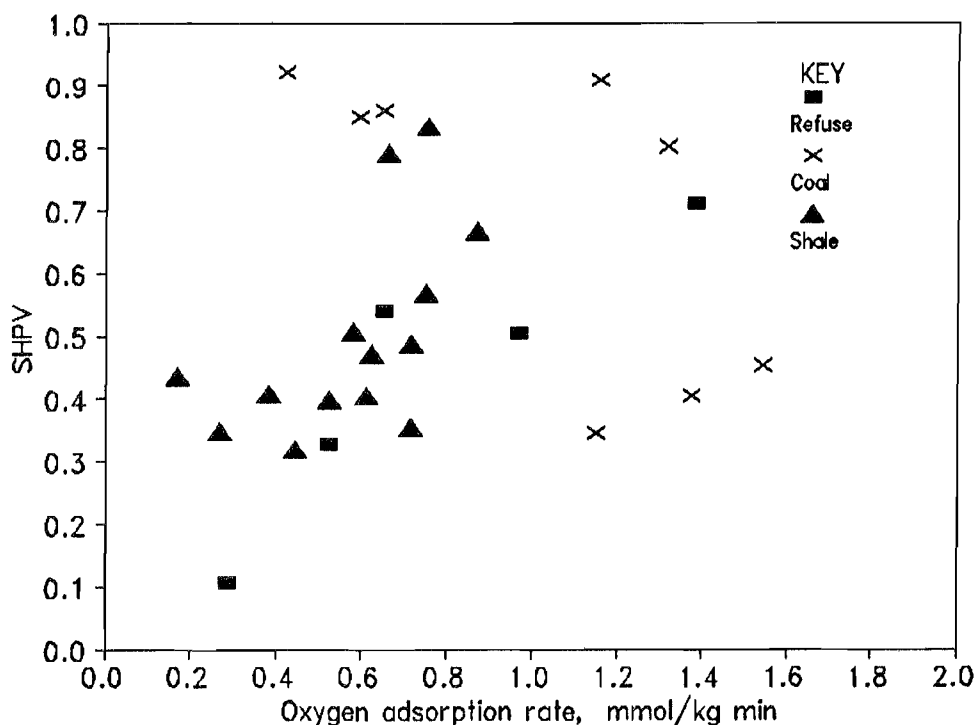
Figure 18

Self-heating probability values versus oxygen reaction mass rate.

Figure 19

Self-heating probability values versus rate of oxygen adsorption.

Figure 20



Self-heating probability values versus rate of oxygen adsorption.

SUMMARY

The results of the study on the self-heating characteristics of coal and other carbonaceous materials demonstrated that measured experimental parameters can be related to potential self-heating. It has also shown that high ash samples, such as coal wastes and carbonaceous shales, are capable of generating sufficient heat to initiate fires in abandoned mines and waste banks.

Data from the study indicate that self-heating is a complex process involving both chemical reactions and factors that control the rates of heat gain and heat loss. In any sample, more than one heat generating reaction may occur, with one reaction providing the activation energy for subsequent reactions. When CO_2 , CO , and O_2 are calculated as moles of gas per gram of coal, the increase in CO_2 and CO are not directly proportional to the decrease in O_2 .

In this group of samples, the concentration of ash was the compositional variable most strongly correlated to self-heating behavior. No correlation between the degree of self-heating and chemical characteristics of the samples was observed. Although the system used did not directly measure the oxidation of pyrite, the probability of self-heating was not correlated to the concentration of

total sulfur in the samples. On a molar basis, there was no correlation between oxygen depletion and sulfur concentration.

In summary, the results of this study indicate that self-heating of coal and carbonaceous materials is a complex process that may involve more than one heat-generating reaction. In addition to the amount of heat generated, factors that control the rates of heat gain and heat loss significantly affect the probability that a coal will self-heat. The results of this study indicate no consistent effect with respect to moisture. At elevated temperatures, the adsorption of moisture may increase the kinetic energy of the sample. Moist air may also adsorb more energy than dry air, effectively removing energy from the system.

By measuring the rate at which the samples approached a preset temperature and the difference between the sample temperature and furnace temperature, then converting these to cumulative probability distributions, a self-heating probability value (SHPV) was calculated that corresponded with the samples observed self-heating behavior. Self-heating was not limited to the coal samples, but was also observed with the shale and refuse samples.

REFERENCES

1. Chaiken, R. F., R. J. Brennan, B. S. Heisey, A. G. Kim, W. T. Malenka, and J. T. Schimmel. Problems in the Control of Anthracite Mine Fires: A Case Study of the Centralia Mine Fire (Aug. 1980), USBM RI 8799, 1983, 93 pp.
2. Kim, A. G., and R. F. Chaiken. Fires in Abandoned Coal Mines and Waste Banks. USBM IC 9352, 1993, 58 pp.
3. Office of Surface Mining, Reclamation and Enforcement (Dep. Interior, Washington, DC). A National Inventory of Abandoned Mine Land Problems: An Emphasis on Health, Safety, and General Welfare Impacts Rep. OSM/TR-4/83, 1983.
4. Dalverny, L. E., and R. F. Chaiken. Mine Fire Diagnostics and Implementation of Water Injection With Fume Exhaustion at Renton, PA. USBM RI 9363, 1991, 42 pp.
5. Schopf, J. M. Definitions of Peat and Coal and of Graphite That Terminates the Coal Series (Graphocite). *J. of Geol.*, v. 74, No. 5, 1966, pp. 584-592.
6. American Society for Testing and Materials. Standard Classification of Coals by Rank. D 388-82 in 1983 Annual Book of ASTM Standards: Petroleum Products, Lubricants, and Fossil Fuels, 1983.
7. Jones, J. R., and B. Cameron. Modern Coastal Back-Barrier Environment: Analog for Coal Basin Carbonaceous Black Shale. *Geology*, v. 16, 1988, pp. 345-348.
8. Chaiken, R. F. In Situ Combustion of Coal for Energy, USBM TPR 84, 1974, 12 pp.
9. Kanury, A. M. Introduction to Combustion Phenomena. Gordon and Breach Sci. Publ., NY, 1975, 411 pp.
10. Smith, A. C., and C. P. Lazarra. Spontaneous Combustion Studies of U.S. Coals. USBM RI 9079, 1987, 28 pp.
11. Kim, A. G. Laboratory Studies on Spontaneous Heating of Coal: A Summary of Information on the Literature. USBM IC 8756, 1977, 13 pp.
12. Smothers, W. J., and Y. Chiang. Handbook of Differential Thermal Analysis. Chemical Publ. Co., Inc., NY, 1966, 633 pp.
13. Knapstein, H. H., K. J. Guterman, and F. H. Franke. Laboratory Experiments on a Controlled Spontaneous Ignition. Proc. 14th Ann. Underground Coal Gasification Symp., Aug. 15-18, 1988, Chicago, IL, DOE/METC-88/6097, pp. 107-113.
14. Singer, J. M., and R. P. Tye. Thermal, Mechanical, and Physical Properties of Selected Bituminous Coals and Cokes. USBM RI 8364, 1979, 37 pp.
15. Grossman, S. L., S. David, and H. Cohen. Evolution of Molecular Hydrogen During the Atmospheric Oxidation of Coal. *Fuel*, 1991, v. 70, pp. 897-898.

APPENDIX.—NOMENCLATURE AND EQUATIONS

The following terms are used to identify variables and in calculations:

T_{f1} Furnace temperature at set point 1 , °C.

T_{s1} Sample temperature at set point 1 , °C.

1 Furnace temperature set point,

$1 = 100$ °C,

$2 = 150$ °C,

$3 = 200$ °C.

$TEMP_1 = (T_s - T_f)_1$, °C.

Maximum temperature difference between furnace and sample at furnace set point 1 .

$TEMP_c$ = Temperature differential calculated from equations 2 and 3.

CPV_{TEMP} = Cumulative probability value based on $TEMP$.

$RATE_1 = (dT_s/dt)_1$, °C/h,

where $RATE_1$ is the change in sample temperature with time at a given furnace set point.

$RATE_c$ = Rate calculated from equation 1.

CPV_{RATE} = Cumulative probability value based on $RATE$.

$SHPV$ = Mean of CPV_{RATE} and CPV_{TEMP} .